Fyn Tyrosine Kinase Regulates the Surface Expression of Glycosylphosphatidylinositol-linked Ephrin via the Modulation of Sphingomyelin Metabolism*

Atsushi Baba[‡1,2], **Koshiro Akagi**[‡1], **Mai Takayanagi**[‡], **John G. Flanagan**[§], **Toshihide Kobayashi**[¶], **and Mitsuharu Hattori**[‡]

From the [‡]Department of Biomedical Science, Graduate School of Pharmaceutical Sciences, Nagoya City University, 3-1 Tanabe-dori, Mizuho-ku, Nagoya, Aichi 467-8603, Japan, the [§]Department of Cell Biology and Program in Neuroscience, Harvard Medical School, Boston, Massachusetts 02115, and the [¶]Supra-Biomolecular System Research Group, RIKEN Frontier Research System, Wako-shi, Saitama 351-0198, Japan

Glycosylphosphatidylinositol-linked ephrin-As play important roles in various biological events, such as neuronal development and immune responses. Because the surface amount of ephrin-As is critical in these events, the trafficking of ephrin-As must be regulated by intracellular machinery. In particular, Src family protein-tyrosine kinases regulate the intracellular trafficking of several membrane molecules and act downstream of ephrin-As; whether they affect the trafficking of ephrin-As, however, has remained unexplored. Here, we report that the activity of Src family protein-tyrosine kinases, particularly Fyn, negatively regulates the cell-surface amount of ephrin-As. The expression of constitutively active Fyn decreases the surface amount of ephrin-As. Conversely, the expression of dominant-negative Fyn or the application of a Src-family inhibitor increases the surface amount of ephrin-A2. The total cellular amount of ephrin-A is inversely correlated with its amount on the surface, suggesting that ephrin-As are more stable in the intracellular compartment. The expression of constitutively active Fyn increases the amount of sphingomyelin clusters on the plasma membrane, whereas inhibiting Fyn decreases it. Moreover, the inhibition of sphingomyelin synthesis greatly increases the surface amount of ephrin-As. Altogether, these results suggest that Fyn regulates the surface amount of ephrin-As by modulating the metabolism of sphingomyelin, which presumably inhibits the trafficking of ephrin-As from endosomes to the plasma membrane. The signaling cascade described here may function as part of the negative feedback loop of ephrin-A function.

Ephrins are the ligands of Eph receptor tyrosine kinases, and these molecules play central roles in many physiological and pathological events, such as neuronal development, adult brain function, angiogenesis, cancer, and immune responses (1, 2). Ephrins are structurally classified into two subclasses: eph-

rin-As are tethered to the outer leaflet of the plasma membrane via glycosylphosphatidylinositol (GPI)[3] linkage, whereas ephrin-Bs are single transmembrane proteins. Ephrin-As and -Bs bind to EphAs and EphBs, respectively, with some exceptions (1, 2). The net concentration of functional ephrins (*i.e.* those on the plasma membrane) is important, a fact that is best exemplified by the mechanism of retinal axon guidance (3, 4).

The amount of ephrin-A protein is regulated at the transcriptional level (4, 5), but such regulation by itself is insufficient to achieve the tight regulation of ephrin concentration on the plasma membrane. In fact, the surface expression of many membrane receptor and ligand molecules is regulated at the posttranslational level by intracellular signaling cascades. For example, during the oocyte meiotic maturation of nematode *Caenorhabditis elegans*, the endocytosis of the Eph receptor is controlled both by intracellular adaptor proteins and by G protein signaling (6). The intracellular trafficking of Notch receptor and its ligand molecules are regulated by several proteins (7), ensuring the signaling capacity of the system. On the other hand, the mechanism by which intracellular signaling cascades affect the surface amount of ephrins remains largely unexplored.

Ephrin-A proteins, like many other GPI-linked proteins, are localized to the so-called "lipid-raft" microdomain on the plasma membrane (8), although the definition, size, biochemical nature, biophysical properties, and physiological importance of such microdomains are still matters of debate (9, 10). Whether the amount and localization of such microdomains are spatiotemporally regulated in neuronal cells remains unknown. Conceivably, the surface expression and/or distribution of ephrin-A is influenced, or even governed, by the amount and/or localization of the lipid rafts. Moreover, ephrin-A is not merely a ligand but also functions as a "receptor" of the EphA "ligand" in a phenomenon called "reverse signaling" (1, 2). In

---

[3] The abbreviations used are: GPI, glycosylphosphatidylinositol; AP, alkaline phosphatase; ApoER2, apolipoprotein E receptor 2; APP, amyloid precursor protein; CA, constitutively active; DN, dominant-negative; FB₁, fumonisin B₁; HmV-NT-Lys, His₆- and monomeric Venus-tagged non-toxic lysenin; HRP, horseradish peroxidase; NPP6, nucleotide pyrophosphatase/phosphodiesterase 6; PP2, 4-amino-5-(4-chlorophenyl)-7-(*t*-butyl)pyrazolo[3,4-*d*]pyrimidine; PP3, 4-amino-7-phenylpyrazol[3,4-*d*]pyrimidine; RFP, red fluorescent protein; SFK, Src-family tyrosine kinase; SM, sphingomyelin; PBS, phosphate-buffered saline.

particular, the binding of the ectodomain of EphA to ephrin-A activates Fyn, a member of the Src-family tyrosine kinases (SFKs), in ephrin-A-bearing cells (11) via the p75 neurotrophin receptor (12). Recently, Fyn activity was reported to modulate the intracellular trafficking of TrkB, a receptor for brain-derived neurotrophic factor (13). Fyn induces the translocation of TrkB into the intracellular lipid-raft fraction (13). SFK is also involved in the intracellular trafficking of epidermal growth factor receptors (14–16), Reelin receptor apolipoprotein E receptor 2 (ApoER2) (17), and vascular endothelial growth factor receptor (18). However, whether Fyn activity affects the intracellular trafficking of ephrin-A is still unknown.

In the present study, we analyzed the effect of Fyn activity on the intracellular trafficking of ephrin-A protein. We report that Fyn activity negatively regulates the surface amount of ephrin-A. Moreover, this effect of Fyn is mediated by the metabolism of sphingomyelin (SM), a major component of the lipid raft microdomain and a regulator of intracellular trafficking. These results led us to hypothesize a novel model regarding the regulatory mechanism of ephrin-A and its downstream signaling.

EXPERIMENTAL PROCEDURES

Expression Vectors—The expression vectors for Myc-tagged ephrin-A2 and ephrin-A5 were described previously (19). The expression vectors for the Fyn mutants (20, 21) were a generous gift from Professor Tadashi Yamamoto (University of Tokyo, Japan). The expression vector for His$_6$- and monomeric Venus-tagged non-toxic lysenin (HmV-NT-Lys) was described previously (22). The expression vector for nucleotide pyrophosphatase/phosphodiesterase 6 (NPP6) was a generous gift from Prof. Junken Aoki (Tohoku University, Japan). The expression vector for red fluorescent protein (RFP, DsRed-Express) was purchased from Clontech-Takara Bio (Mountain View, CA).

Antibodies and Reagents—Anti-Myc mouse monoclonal antibody (9E10) and anti-β-actin mouse monoclonal antibody (AC-15) were purchased from Sigma. Anti-caveolin-1 rabbit polyclonal antibody (N-20) and anti-flotillin-1 rabbit polyclonal antibody (H-104) were purchased from Santa Cruz Biotechnologies (Santa Cruz, CA). Horseradish peroxidase (HRP)-conjugated secondary antibodies and HRP-streptavidin were purchased from Amersham Biosciences. Alexa-Fluor594-conjugated secondary antibody was purchased from Invitrogen. Fumonisin B$_1$ (FB$_1$), 4-amino-5-(4-chlorophenyl)-7-(*t*-butyl)pyrazolo[3,4-*d*]pyrimidine (PP2), and 4-amino-7-phenyl-pyrazol[3,4-*d*]pyrimidine (PP3) were purchased from Merck Biosciences (Darmstadt, Germany). *N*-Hexanoyl-*d*-sphingoshine (C$_6$-ceramide) and sphingomyelin were purchased from Sigma.

Cell Culture and Transfection—COS-7 cells were maintained in Dulbecco's modified Eagle's medium containing 10% fetal calf serum (Equitech-Bio, Kerrville, TX) and antibiotics. Transfection was performed using Lipofectamine 2000 (Invitrogen), according to the manufacturer's protocol.

Quantification of the Surface Amount of Ephrin-A Using EphA3-alkaline Phosphatase Fusion Protein—Culture supernatant containing EphA3-alkaline phosphatase (AP) was obtained, and the binding assay was performed as reported previously (23). Briefly, the cells were incubated with EphA3-AP

for 60 min, washed five times with Hanks' balanced salt solution containing 0.5 mg/ml bovine serum albumin, 0.1% NaN$_3$, and 20 mM HEPES, pH 7.2, treated for 2 min with an acetone-formalin fixative (60% acetone, 8% formalin, 20 mM HEPES, pH 7.2), washed two times in HEPES-buffered saline (150 mM NaCl, 20 mM HEPES, pH 7.2), and then incubated at 65 °C for 30 min to inactivate the endogenous AP activity. After rinsing twice with AP buffer (5 mM MgCl$_2$, 100 mM NaCl, 100 mM Tris-HCl, pH 9.5), the cells were stained with 0.17 mg/ml 5-bromo-4-chloro-3-indolyl phosphate and 0.33 mg/ml of nitro blue tetrazolium in AP buffer. The reactions were stopped by changing the solution to phosphate-buffered saline (PBS) containing 20 mM EDTA. Microscopic images were captured using a color-cooled charge-coupled device camera and a VB-6000 image control system (Keyence, Osaka, Japan) equipped with a SZX7 stereoscopic microscope (Olympus, Tokyo, Japan).

Western Blotting—Samples were separated by 12% SDS-PAGE and transferred onto a polyvinylidene difluoride membrane. The blotted membranes were blocked with 5% skimmed milk in Tris-buffered saline with 0.05% Tween 20 (TBST) for 1 h and incubated with the primary antibody for 2 h. After washing four times with TBST, the membranes were incubated with HRP-conjugated secondary antibody (1:4000) for 1 h and washed, and the labeled proteins were detected using Immobilon Western Chemiluminescent HRP Substrate (Millipore, Bedford, MA). Images were captured using a LAS3000mini system (Fuji, Tokyo, Japan).

Biotinylation of Cell-surface Proteins—Biotinylation of the cell-surface proteins was performed as described previously (24) with some modifications. Twenty-four hours after transfection, COS-7 cells were rinsed with ice-cold PBS and incubated with 0.125 mg/ml of sulfo-NHS-biotin (Thermo Scientific, Rockford, IL) for 30 min at 4 °C. After washing twice with PBS containing 100 mM glycine to stop the reaction, the cells were lysed with radioimmune precipitation assay buffer (10 mM phosphate buffer, pH 7.4, 150 mM NaCl, 2 mM EDTA, 1% sodium deoxycholate, 0.1% SDS, 1% Triton X-100). The lysates were recovered and centrifuged at 15,000 × g for 2 min at 4 °C to remove debris. The supernatant was then incubated with streptavidin-conjugated agarose (Sigma) and rotated for 60 min at 4 °C. After centrifugation at 3,300 × g for 1 min, the supernatants were removed and the resins were washed six times with radioimmune precipitation assay buffer and eluted with SDS-PAGE sampling buffer (62.5 mM Tris-HCl, pH 6.8, 2% SDS, 5% β-mercaptoethanol, 10% glycerol, and 0.05% bromphenol blue).

Detection of SM Clusters in Situ—HmV-NT-Lys protein was expressed in *Escherichia coli* BL21-CodonPlus-RP (Stratagene, La Jolla, CA) and purified using nickel-nitrilotriacetic acid-agarose (Qiagen, Valencia, CA), according to the manufacturer's protocol. HmV-NT-Lys solutions were diluted in PBS containing 2% bovine serum albumin. To detect the SM clusters *in situ*, the cells were fixed and incubated with 1–2 µg/ml HmV-NT-Lys for 1.5–3 h and washed with PBS four times. The fluorescent images were captured using a BZ-9000 digital fluorescence microscope (Keyence).

Immunocytochemistry—The cells were fixed with 4% paraformaldehyde for 10 min or with 4% formaldehyde for 5 min at room temperature. After washing with PBS twice, the cells were permeabilized with PBS containing 0.05% Tween 20 for 30 min and then blocked by incubation with PBS containing 2% bovine serum albumin for 30 min. The cells were then incubated with the primary antibody for 2 h at room temperature, washed four times with PBS, incubated with the secondary antibody for 90 min, and washed four times with PBS and twice with water. To visualize the nucleus, 2 μg/ml Hoechst 33342 (Invitrogen) was added to the secondary antibody solution. Fluorescent images were captured using a BZ-9000 digital fluorescence microscope. In the case of optical sectioning, the samples were examined using an LSM510meta confocal laser-scanning microscope (Carl Zeiss, Tokyo, Japan).

Sphingolipid Depletion and Repletion—The cells were depleted of SM by growing them in the presence of 40 μg/ml FB$_1$ for 48 h. For repletion, 5 μM C$_6$-ceramide was simultaneously added to the FB$_1$-containing culture media.

Lipid Extraction and Analysis Using TLC—Prior to the phospholipid analysis, COS-7 cells were preincubated with medium containing 5 μM PP2 or PP3 for 24 h. After washing with PBS twice, the cells were lysed under a hypotonic condition containing 0.1 M acetic acid. The cellular total lipids were extracted according to the method described by Bligh and Dyer (25). Aliquots of the extracts were analyzed using TLC on silica gel 60 TLC plates (Amersham Biosciences) using a running solvent composed of chloroform:methanol:water at a ratio of 25:15:2. Phospholipid spots were visualized by spraying with Dittmer's reagent (26).

Quantification and Analysis of Fluorescent Intensities—For the fluorometric assays, the mean fluorescent intensity was scored using ImageJ analysis software, version 1.41m (rsbweb.nih.gov/ij/). Images were captured using a BZ-9000 digital fluorescence microscope (Keyence) with a 20× objective, and individual cells in 10–15 randomly selected microscopic fields were traced. Dividing or dead cells were excluded from the measurements based on the Hoechst staining patterns. To calculate the staining intensity of HmV-NT-Lys, the RFP-expressing area in each cell was outlined using an automated program and was defined as the whole cell region. The mean fluorescence intensity of the HmV-NT-Lys image in the corresponding region was calculated by subtracting the background and was expressed as 256 gradations. To calculate the mean fluorescence intensity of surface Myc-ephrin-A2, the optically observed area of each cell was defined as the whole cell region, and the mean fluorescence intensity of the Myc-immunoreactive images was calculated. All measurements from two independent experiments were performed in a blinded manner.

Statistical Analysis—Multiple group comparisons among each group were made using the Scheffé F-test after one-way analysis of variance. The values are expressed as the mean ± S.D. Differences were considered significant at $p < 0.05$.

RESULTS

Modulation of Fyn Activity Affects the Surface Amount of Ephrin-A—COS-7 cells were transiently transfected with the expression vector for Myc-ephrin-A2 together with that for dominant negative Fyn (Fyn-DN), that for constitutively active Fyn (Fyn-CA), or pcDNA3.1 (control). Twenty-four hours after transfection, the cells were stained with EphA3-AP to assess the surface amount of Myc-ephrin-A2. When Fyn-DN was co-transfected, the surface amount of Myc-ephrin-A2 increased, compared with that of the control (Fig. 1, *B* and *A*, respectively). On the other hand, the co-expression of Fyn-CA dramatically reduced the surface amount of Myc-ephrin-A2 (Fig. 1*C*). Staining with the control AP gave no signal in the Myc-ephrin-A2-transfected cells (Fig. 1*K*). These results indicate that Fyn activity negatively regulates the surface amount of Myc-ephrin-A2. To verify the role of Fyn on the surface expression of other types of GPI-linked ephrin-A, Myc-ephrin-A5 was expressed in COS-7 cells either with pcDNA3.1, Fyn-DN, or Fyn-CA. EphA3-AP staining clearly revealed that the surface amount of Myc-ephrin-A5 increased when the cells were co-transfected with Fyn-DN (Fig. 1*E*) and decreased when the cells were co-transfected with Fyn-CA (Fig. 1*F*). The cells expressing Myc-ephrin-A5 were not stained by control AP (Fig. 1*L*). These results indicate that a common mechanism exists for regulating the surface amount of Myc-ephrin-A2 and Myc-ephrin-A5.

We next checked whether the inhibition of endogenous SFK activity was sufficient for increasing the surface amount of Myc-ephrin-As. COS-7 cells expressing either Myc-ephrin-A2 or Myc-ephrin-A5 were incubated with 5 μM PP2, an SFK inhibitor, for 24 h and then stained with EphA3-AP. As a control, the cells were incubated with PP3, an inactive analogue of PP2. The surface amount of Myc-ephrin-A2 in the PP2-treated cells was more abundant than that in the PP3-treated cells (Fig. 1, *H* and *G*, respectively). The same tendency was observed in cells expressing Myc-ephrin-A5 (Fig. 1, *J* and *I*). Thus, these results indicate that the surface amounts of Myc-ephrin-As are regulated by the endogenous SFK activity.

Fyn Activity Modulates the Surface Amount of Ephrin-A by Altering Its Intracellular Sorting—By which mechanism does SFK regulate the surface amount of ephrin-A? We first speculated that SFK simply regulates the total amount of ephrin-A protein in the cell. To test this hypothesis, COS-7 cells were transfected with the expression vector for Myc-ephrin-A2 together with pcDNA3.1 (control), Fyn-DN, or Fyn-CA, and whole cell lysates were prepared 24 h later. These lysates were then analyzed using SDS-PAGE and Western blotting with anti-Myc antibody (Fig. 2*A*, *top panel*, *lanes 1–3*). Quite surprisingly, the co-expression of Fyn-DN greatly decreased the total amount of Myc-ephrin-A2 (Fig. 2*A*, *top panel*, *lane 2*), whereas the expression of Fyn-CA increased it (Fig. 2*A*, *top panel*, *lane 3*). In other words, the total amount of Myc-ephrin-A2 in the cells expressing Fyn mutants was inversely correlated with the surface amount of Myc-ephrin-A2 (Fig. 1, *A–C*). The amounts of caveolin-1 and flotillin-1, two proteins that are localized to the "lipid raft," did not change (Fig. 2*A*, *middle panels*, *lanes 1–3*). The amounts of β-actin were also unaffected (Fig. 2*A*, *bottom panel*, *lanes 1–3*). Likewise, the expression of Fyn-DN and Fyn-CA decreased and slightly increased the total amount of Myc-ephrin-A5, respectively (Fig. 2*A*, *top panel*, *lanes 5* and *6*, respectively), without affecting the amounts of caveolin-1, flotillin-1, or β-actin (Fig. 2*A*, *lanes 4–6*).
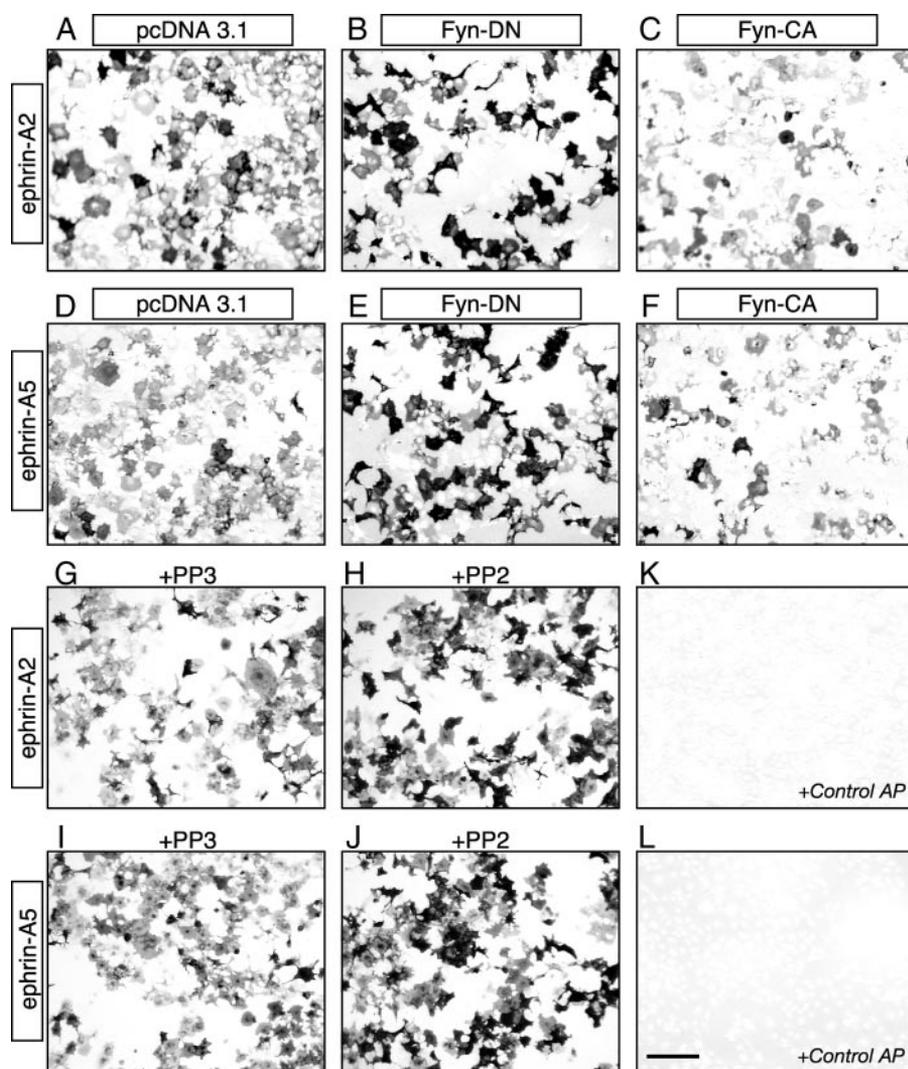
FIGURE 1. **Fyn activity modulates the cell surface amount of ephrin-As.** *A–F*, COS-7 cells were transfected with expression vectors for Myc-ephrin-A2 (*A–C*) or -A5 (*D–F*) together with pcDNA3.1 (*A* and *D*), Fyn-DN (*B* and *E*), or Fyn-CA (*C* and *F*). Twenty-four hours after transfection, the cells were incubated with EphA3-AP, fixed, washed, and stained for bound AP activity. *G–J*, COS-7 cells expressing Myc-ephrin-A2 (*G* and *H*) or -A5 (*I* and *J*) were incubated with 5 μM of PP3 (*G* and *I*) or PP2 (*H* and *J*) for 24 h. The cells were then stained with EphA3-AP. *K* and *L*, COS-7 cells were transfected with the expression vector for Myc-ephrin-A2 (*K*) or -A5 (*L*) and stained with the control AP. *Scale bar*: in *L* (for *A–L*), 100 μm.

ing the intracellular sorting of ephrin-A protein. It is also suggested that ephrin-As in the intracellular compartment are more stable than those on the plasma membrane, because the total amounts of Myc-ephrin-As were more abundant in cells that have them mostly in the intracellular compartment (*i.e.* Fyn-CA-expressing cells, Fig. 2*A*, *lanes 3* and *6*) than in cells with Myc-ephrin-As on the plasma membrane (*i.e.* Fyn-DN-expressing cells, Fig. 2*A*, *lanes 2* and *5*).

The cellular distribution of ephrin-A2 was also examined by immunostaining. Cells expressing Myc-ephrin-A2 alone (Fig. 3*A*), with Fyn-DN (Fig. 3*B*), or with Fyn-CA (Fig. 3*C*) were fixed and stained with anti-Myc antibody without permeabilization to detect the surface Myc-ephrin-A2. Under these conditions, the total fluorescence signal was higher in the Fyn-DN-transfected cells (Fig. 3*B*) and lower in the Fyn-CA-transfected cells (Fig. 3*C*) than that in the control cells (Fig. 3*A*). Then, we next compared the intracellular localization of Myc-ephrin-A2 by immunostaining after membrane permeabilization. As shown in Fig. 3*D*, Myc-ephrin-A2 protein was distributed mostly along the edge of the cell, the putative cell-surface region, and was also diffusely present in the cytoplasmic region. In cells co-expressing Fyn-DN, the fluorescence signals at the edge of the cell were augmented, whereas those in the intracellular region were diminished (Fig. 3*E*). In cells co-expressing Fyn-CA, on the other hand, the cell-surface signals were diminished and signals were often found throughout the cytoplasm, distributed in apparently clustered and punctate manner (Fig. 3*F*, *arrowheads*), indicating that Myc-ephrin-A2 protein tends to be retained within the cell when Fyn activity is high. These results thus strongly suggest that Fyn activity affects the surface expression of Myc-ephrin-A2 by selectively changing the intracellular trafficking of this protein.

Fyn Regulates the Cellular SM Level and Clustering— We next investigated whether SFK activity can modulate the amount or localization of the lipid-raft microdomain on the plasma membrane, where ephrin-As are thought to localize. For this purpose, COS-7 cells were transfected with either pcDNA3.1, Fyn-DN, or Fyn-CA followed by staining with HmV-NT-Lys, which binds specifically to SM clusters (22, 27). The shape of each transfected cell was simultaneously visual-

We next asked whether the surface amounts of other proteins were affected by modulating Fyn activity. For this purpose, the cells were transfected with expression vectors for Myc-ephrin-A2 and either pcDNA3.1, Fyn-DN, or Fyn-CA, and the cell-surface proteins were labeled with sulfo-NHS-LC-biotin. The biotinylated proteins were precipitated using streptavidin-conjugated agarose, followed by Western blotting analysis. When transfected with Fyn-DN, Myc-ephrin-A2 protein in the biotinylated (cell surface) fraction increased (Fig. 2*B*, *lane 2*), whereas that in the corresponding fraction of Fyn-CA co-transfected cells decreased (Fig. 2*B*, *lane 3*), confirming the results of EphA3-AP staining (Fig. 1, *A–C*). On the other hand, the expression of the Fyn mutants hardly affected the surface amounts of most of the other cellular proteins (Fig. 2*B*, *lanes 4–6*), as assessed by detection with HRP-streptavidin. These results suggest that the surface amount of ephrin-As is selectively regulated by SFK activity, which is achieved by modulat-

FIGURE 2. **Fyn activity alters the sorting machinery of ephrin-As.** *A*, COS-7 cells were transfected with Myc-ephrin-A2 (*lanes 1-3*) or -A5 (*lanes 4-6*) together with pcDNA3.1 (*lanes 1* and *4*), Fyn-DN (*lanes 2* and *5*), or Fyn-CA (*lanes 3* and *6*), respectively. A representative immunoblot of the protein levels of Myc-ephrin-As (*top panel*), caveolin-1, flotillin-1, and β-actin (*bottom panel*) in the total cell lysates is shown. The *black bar* indicates the positions of Myc-ephrin-A2. Transfection with Fyn-DN or Fyn-CA caused a decrease or an increase in Myc-ephrin-As without affecting caveolin-1, flotillin-1, and β-actin. *B*, COS-7 cells were transfected with the indicated vectors, and their cell-surface proteins were labeled with sulfo-NHS-LC-biotin. The cells were then lysed, and the labeled proteins were precipitated with streptavidin beads, followed by SDS-PAGE and Western blotting using anti-Myc antibody (*lanes 1-3*). The *black bar* indicates the positions of Myc-ephrin-A2. Total biotinylated proteins were visualized using streptavidin-HRP (*lanes 4-6*). The positions of the molecular weight mass (kDa) markers are shown to the *left* of the *panel*.

FIGURE 3. **Fyn activity alters the subcellular distribution of ephrin-A2.** *A–C*, COS-7 cells were co-transfected with Myc-ephrin-A2 and with the indicated Fyn mutants, then fixed and immunostained with anti-Myc antibody without membrane permeabilization. *Scale bar*: in *C* (for *A–C*), 200 μm. *D–F*, intracellular distribution of Myc-ephrin-A2 in pcDNA3.1 (*D*)-, Fyn-DN (*E*)-, or Fyn-CA (*F*)-transfected cells. Twenty-four hours after transfection, COS-7 cells were permeabilized and immunostained with anti-Myc antibody. Confocal laser optical sectioning (1 μm thick) was used to visualize the distribution of Myc-ephrin-A2 in the transfected cells. The *arrowheads* in *F* indicate the intracellular Myc-ephrin-A2 puncta in Fyn-CA-transfected cells. *Scale bar*: in *F* (for *D–F*), 10 μm.

ized using the fluorescence of co-expressed RFP. The SM clusters in the control COS-7 cells were localized rather diffusely (Fig. 4, *A* and *D*). In cells expressing Fyn-DN, the amount of SM clusters decreased, compared with that in the control cells (Fig. 4, *B* and *E*). In contrast, cells expressing Fyn-CA had large and/or abundant SM clusters (Fig. 4, *C* and *F*). As shown in Fig. 4*G*, the fluorescence intensity of the HmV-NT-Lys signals significantly decreased in Fyn-DN-transfected cells and increased in Fyn-CA-transfected cells: the averages of the mean intensities were 60.2 ± 23.3 (pcDNA3.1), 38.6 ± 18.9 (Fyn-DN), and 98.8 ± 50.7 (Fyn-CA), respectively. Thus, Fyn activity positively regulates the amount of SM clusters on the plasma membrane. To test whether endogenous SFK activity modulates the cellular SM levels and clusters, we applied PP2 or PP3 to COS-7 cells

and stained them with HmV-NT-Lys. Consequently, the amount of SM clusters markedly decreased when the cells were treated with PP2 but not with PP3 (Fig. 4, *I* and *H*, respectively). Concomitantly, the total cellular SM amount was much lower in the PP2-treated cells (Fig. 4*J*, *lane 4*) than in the PP3-treated cells (Fig. 4*J*, *lane 3*). Thus, SFK activity modulates the cellular SM level and clustering.

We next compared the localization of Myc-ephrin-A2 and SM in the Fyn-CA-expressing cells by combining immunocytochemistry and HmV-NT-Lys staining after membrane permeabilization. As shown in Fig. 5*A*, many clusters or vesicles of Myc-ephrin-A2 were observed when Fyn-CA was co-expressed. Interestingly, few of these clusters or vesicles overlapped with the SM clusters (Fig. 5, *C* and *D*) within the cells. Thus, although Myc-ephrin-A2 and SM may be located in the same microdomain on the plasma membrane, they are segregated to within the intracellular compartment of Fyn-CA-expressing cells.

Cell-surface Amount of Ephrin-A Is Regulated by SM—We next explored the possibility that a change in the amount of SM might affect the surface amount of ephrin-A2. To alter the cellular sphingolipid levels, the cells were treated with FB$_1$, which inhibits sphingosine *N*-acyltransferase (28). FB$_1$ reduces sphingolipid biosynthesis without affecting cellular cholesterol levels, and the addition of C$_6$-ceramide to FB$_1$-treated cells restores the cellular sphingolipid levels (29). COS-7 cells expressing Myc-ephrin-A2 were incubated with FB$_1$ in the presence or absence of C$_6$-ceramide and were stained with HmV-NT-Lys (Fig. 6, *A–C*) or with EphA3-AP (Fig. 6, *D–F*). Under the control conditions, the COS-7 cells were brightly stained by HmV-NT-Lys (Fig. 6*A*). When treated with FB$_1$, the amount of SM clusters was greatly reduced in most of the cells (Fig. 6*B*). This effect was partly restored in the presence of C$_6$-ceramide (Fig. 6*C*). In the FB$_1$-treated cells, the surface
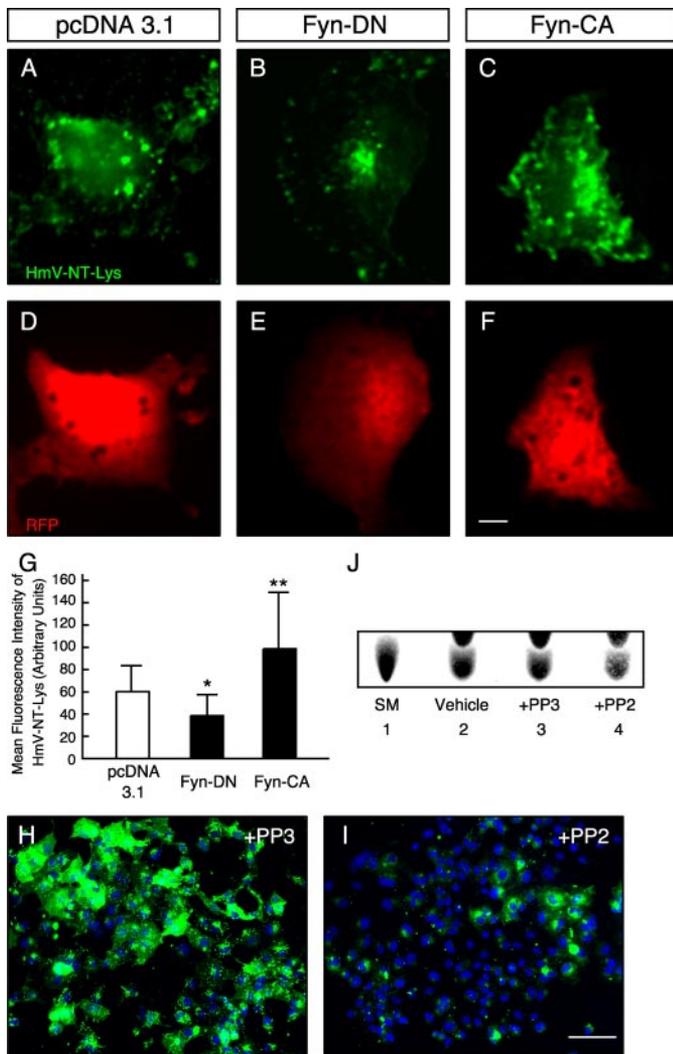
FIGURE 4. **Fyn activity regulates the amount and the clustering of SM.** *A–F*, COS-7 cells were transfected with expression vectors for pcDNA3.1 (*A* and *D*), Fyn-DN (*B* and *E*), or Fyn-CA (*C* and *F*) together with RFP. Twenty-four hours after transfection, the cells were fixed and stained with HmV-NT-Lys (*A–C*; *green*). The fluorescence of RFP reveals the cell shape (*D–F*; *red*). *Scale bar*: in *F* (for *A–F*), 10 μm. *G*, summary of the effects of pcDNA3.1, Fyn-DN, and Fyn-CA on the content of the SM clusters in COS-7 cells. The pixel intensity of HmV-NT-Lys fluorescence was measured in each cell, and the average of the mean fluorescence intensity is represented. *, $p < 0.05$; **, $p < 0.01$ *versus pcDNA3.1*: Scheffé F-test after one-way analysis of variance ($n = 44\text{–}46$ cells from two independent experiments). *H* and *I*, COS-7 cells were maintained in media containing 5 μM of PP3 (*H*) or PP2 (*I*), followed by incubation with HmV-NT-Lys (*green*) and Hoechst 33342 (*blue*). In the presence of PP2, the COS-7 cells showed the reduced binding of HmV-NT-Lys. *Scale bar*: in *I* (for *H* and *I*), 100 μm. *J*, TLC analysis of cellular phospholipids levels in DMSO-, PP3-, or PP2-treated COS-7 cells (*lanes 2, 3,* and *4*, respectively). The total lipids of the COS-7 cells were extracted and separated using TLC. *SM*, sphingomyelin standard (*lane 1*). The representative image shows that PP2 treatment decreased the SM levels.

FIGURE 5. **Intracellular compartments containing ephrin-A2 or SM are segregated in Fyn-CA-expressing cells.** *A–D*, Fyn-CA- and Myc-ephrin-A2-expressing COS-7 cells were stained with anti-Myc antibody (*A*; *red*), Hoechst 33342 (*A*; *blue*) and HmV-NT-Lys (*B*; *green*). The *merged image* is shown in *C*. The intracellular puncta of Myc-ephrin-A2 contained few SM clusters. The *white box* in *C* is magnified in *D*. *Scale bar*: in *A* (for *A–C*), 10 μm.
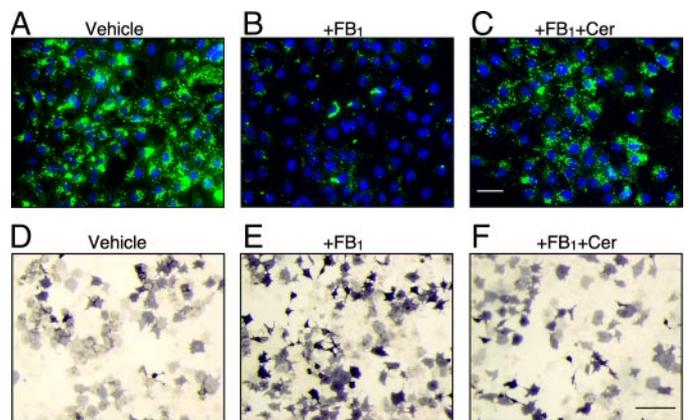
FIGURE 6. **Sphingolipid depletion increases the surface amount of ephrin-A2.** *A–C*, COS-7 cells were maintained in media containing DMSO alone (*A*), 40 μg/ml FB$_1$ (*B*), or 40 μg/ml FB$_1$ and 5 μM of C$_6$-ceramide (*Cer*; *C*) for 48 h, followed by incubation with HmV-NT-Lys (*green*) and Hoechst 33342 (*blue*). The *merged fluorescence* of the HmV-NT-Lys and Hoechst dye images is shown. *Scale bar*: in *C* (for *A–C*), 50 μm. *D–F*, EphA3-AP binding to Myc-ephrin-A2-expressing COS-7 cells depleted of SM. The COS-7 cells were transfected with an expression vector for Myc-ephrin-A2 after preincubated with DMSO alone (*D*), 40 μg/ml of FB$_1$ (*E*), or 40 μg/ml of FB$_1$ and 5 μM of C$_6$-ceramide (*F*) for 24 h and were maintained for another 24 h with the same drugs followed by EphA3-AP staining. *Scale bar*: in *F* (for *D-F*), 100 μm.

amount of Myc-ephrin-A2 greatly increased (Fig. 6*E*), compared with that in control cells (Fig. 6*D*). When C$_6$-ceramide was present, the increase in the surface amount of Myc-ephrin-A2 was less obvious (Fig. 6*F*). Therefore, reducing the cellular sphingolipid level was sufficient to increase the surface amount of Myc-ephrin-A2.

We further addressed the possibility that the regulation of sphingolipid metabolism by Fyn activity may alter the surface amount of ephrin-A. COS-7 cells were transfected with the expression vectors for Myc-ephrin-A2 and either pcDNA3.1 (control) or Fyn-CA in the presence of FB$_1$, and Myc-ephrin-A2 protein on the cell surface was labeled with anti-Myc antibody without membrane permeabilization. The surface amount of Myc-ephrin-A2 was significantly reduced by the co-expression of Fyn-CA (Fig. 7*B*), as previously shown in the experiments described above (Figs. 1–3). When cells expressing Fyn-CA were treated with FB$_1$, however, the surface amount of Myc-ephrin-A2 was increased up to the control level (Fig. 7, *C* and *A*, respectively; data are summarized in *D*), implying that Fyn requires SM for the down-regulation of the surface amount of Myc-ephrin-A2. Thus, Fyn may regulate the intracellular sort-
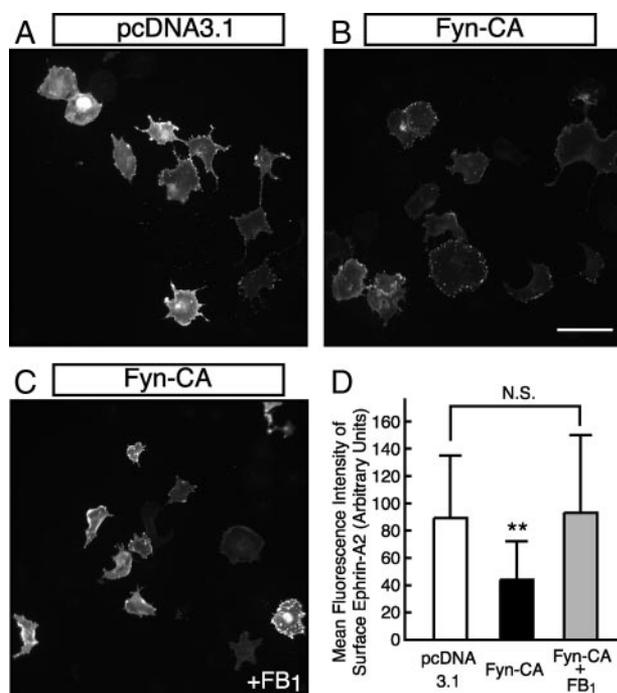
FIGURE 7. **Fyn activity regulates the surface amount of ephrin-A2 by regulating sphingolipid metabolism.** *A–C*, COS-7 cells were maintained in the presence (*C*) or absence (*A* and *B*) of 40 μg/ml FB$_1$ for 24 h. Then the cells were transfected with Myc-ephrin-A2 together with pcDNA3.1 (*A*) or Fyn-CA (*B* and *C*) and were further maintained in the same drugs for 24 h. The cells were fixed and stained with anti-Myc antibody without membrane permeabilization. Representative fluorescent images of Myc-ephrin-A2 are shown. *Scale bar*: in *B* (for *A–C*), 100 μm. *D*, summary of the effect of FB$_1$ on the Fyn-CA-mediated surface amount of Myc-ephrin-A2. The fluorescence intensity of Myc-ephrin-A2 in each cell, as shown in *A–C*, was calculated using ImageJ software. The *ordinate* indicates the average mean intensity of Myc fluorescence without permeabilization. **, $p < 0.01$ *versus* pcDNA3.1, *N.S.*, not significant: Scheffé F-test after one-way analysis of variance (*n* = 41–44 cells from two independent experiments).

ing of Myc-ephrin-A2, at least in part, by modulating sphingolipid metabolism.

DISCUSSION

In this study, we found that Fyn, a member of SFK that acts downstream of the Eph-ephrin reverse signaling pathway (11, 12), regulates the surface amount of ephrin-A by modulating the SM content (or localization) of the cell. This is the first demonstration of the molecular mechanism responsible for the intracellular signaling that regulates the surface amount of ephrin-As at the posttranslational level. The idea that Fyn or SFK affects the localization of a membrane molecule by modulating lipid metabolism is also a novel concept. Recently, Fyn was reported to regulate the surface amounts of amyloid precursor protein (APP) and ApoER2, a receptor for Reelin (17). There are two interesting differences between the effects of Fyn on APP or ApoER2 and those on ephrin-A2. First, the expression of Fyn-CA increases the surface amounts of APP and ApoER2 while it decreases that of ephrin-A. Second, the expression of Fyn-CA significantly increases the total ephrin-A level but has no effect on that of APP or ApoER2 (17). Interestingly, the total amounts of ephrin-A, APP, and ApoER2 are decreased by Fyn-DN (17). APP and ApoER2 contain an intracellular domain that is phosphorylated by Fyn, and they have a number of bind-

ing proteins that can modify their intracellular trafficking (17). Ephrin-As, being GPI-linked proteins, are not subject to such regulation. Therefore, although Fyn regulates the intracellular trafficking of ephrin-A, APP, and ApoER2, the underlying mechanisms of these regulations must differ. The trafficking of APP and ApoER2 is regulated by phosphoinositides (17, 24). It would be interesting to test whether it is also regulated by sphingolipids. We also found that co-expression of Fyn mutants did not affect the surface amount of other structurally unrelated GPI-linked proteins NPP6 and placental alkaline phosphatase (data not shown), suggesting that the action of Fyn is selective, if not specific, to ephrin-A.

Generally, GPI-linked proteins mature in the Golgi apparatus, are transported to the plasma membrane by vesicular trafficking, and are probably constantly internalized via a clathrin-dependent or -independent mechanism (30–33). Internalized GPI-linked proteins are retained in the endosome and are subsequently subjected to degradation or are "recycled" to the plasma membrane (29, 31–34). Our finding that the surface concentration of SM is negatively correlated with that of ephrin-As raises three possibilities. 1) SM inhibits the maturation or transport of ephrin-A. This possibility is rather unlikely, because we did not observe the accumulation of Myc-ephrin-A2 in the Golgi apparatus in Fyn-CA-expressing cells (Figs. 3*F* and 5*A*). 2) SM directly enhances the internalization of ephrin-A. While possible, the observation that intracellular vesicles containing Myc-ephrin-A2 typically do not contain SM clusters (Fig. 5, *C* and *D*) suggests that SM and ephrin-A tend to be segregated in Fyn-CA-expressing cells. 3) SM augments the retention/recycling ratio. Currently, we favor this scenario, because the amount of intracellular ephrin-A is increased in Fyn-CA-expressing (*i.e.* SM-rich) cells (Fig. 2, *A* and *B*), and sphingolipid depletion in Chinese hamster ovary cells reportedly leads to the retention of two GPI-linked proteins, folate receptor, and decay-accelerating factor, in the endosome fraction (29). How SM affects intracellular trafficking of ephrin-As remains to be investigated. It was also suggested that ephrin-As in the intracellular compartment is more stable than those on the plasma membrane (Fig. 2). This may be due to selective proteolysis of ephrin-A on the plasma membrane by a disintegrin and metalloprotease family (19). Whether SM directly regulates the proteolysis or degradation of ephrin-As remains to be investigated.

We hoped to confirm that the results obtained in COS-7 cells could be reproduced in neuronal cells, but such studies were hindered by two technical difficulties. First, although HmV-NT-Lys can reportedly stain cultured neurons (35), neither hippocampal neurons nor cortical neurons produced a significant signal when we stained them using HmV-NT-Lys (data not shown). The reason for the lack of staining is unknown, but the high contents of non-SM sphingolipids in neuronal cells may inhibit the clustering of SM, which is a prerequisite for HmV-NT-Lys binding (27, 36). Second, the overexpression of ephrin-A and Fyn mutants was not satisfactorily obtained in neuronal cells (data not shown), probably because of their toxicity. Thus, in future studies, the quantification of endogenous ephrin-A in knockout mice for Fyn or some other SFK will be necessary.
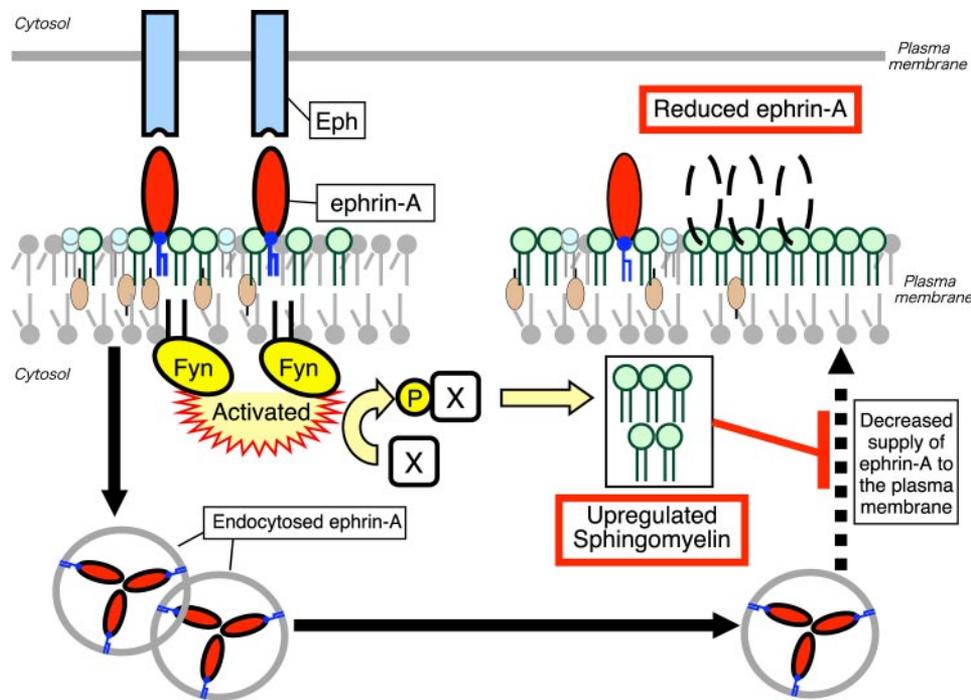
FIGURE 8. **Model of how Fyn activity contributes to Eph-ephrin reverse signaling by regulating the surface amount of ephrin-A.** Ephrin-A is constantly endocytosed to the cytosol and recycled to the plasma membrane. When ephrin-A binds to EphA, reverse signaling is transmitted in the ephrin-A-expressing cells and Fyn is activated. Fyn kinase phosphorylates an unidentified protein ("*X*"), and this leads to an increase in cellular sphingomyelin levels. Changes in the cell-surface sphingomyelin levels prolong the retention time of ephrin-A in the recycling endosomal compartment (29), reducing the surface amount of ephrin-A. This pathway creates a negative feedback loop for Eph-ephrin reverse signaling.

tive feedback of Eph-ephrin reverse signaling; that is, when an ephrin-A-bearing cell encounters EphA-bearing cells, the surface amount of ephrin-A decreases. This phenomenon may be important for preventing the hyperactivation of EphA and/or for terminating signaling in both directions. Moreover, cross-talk with other neuronal signaling pathways can be envisaged. For example, SFK, most likely Fyn, is activated by Reelin in neuronal cells (43, 44). Our results presented here predict that Reelin down-regulates ephrin-A by up-regulating SM. Furthermore, amyloid-β-peptide 42, the most likely causative molecule of Alzheimer disease, is known to down-regulate SM (45), which would increase the surface amount of ephrin-A. Because ephrin-A is one of the most important inhibitors of axonal elongation and regeneration (46), this pathway may be involved in the pathogenesis of Alzheimer disease. Thus, we believe that our present findings contribute significantly not only to the elucidation of questions in basic cell biology, but also to the development of novel therapeutics for neurodevelopmental and neurodegenerative diseases.

How SFK modulates the cellular SM content and/or localization is a daunting question, because our understanding of the regulatory mechanisms underlying the synthesis, transport, and degradation of SM is still quite premature (37–39). There are two isozymes for SM synthase (40), each of which seem to have independent roles (41). To the best of our knowledge, whether the activity of SM synthase is regulated by an intracellular signaling cascade is unknown. However, our result, that an inhibitor of sphingolipid synthesis enabled the recovery of the Fyn-CA-induced decrease in surface ephrin-A2 (Fig. 7), may suggest that activated Fyn can directly up-regulate SM clustering by activating SM synthesis. The regulation of cellular SM amounts by sphingomyelinases is a relatively well studied area (37, 39), but only a few reports have discussed the regulation by phosphorylation. Very recently, Chudakova *et al.* (42) reported that Lyn, an integrin-associated member of SFKs, suppresses the activities of sphingomyelinases. Thus, the up-regulation of SM by SFK via the inhibition of its hydrolysis may be a universal phenomenon. Finally, we could not exclude the possibility that sphingolipids other than SM play a role in the regulation of ephrin-A trafficking.

The model proposed in the present study is summarized in Fig. 8. Ephrin-A, like other GPI-linked proteins, undergoes continuous cycling between the plasma membrane and the intracellular endosome fraction. When ephrin-A binds to EphA, Fyn is activated in ephrin-A-bearing cells. The activation of SFK up-regulates SM via an unknown mechanism, and SM inhibits the transport of intracellular ephrin-A to the plasma membrane. Therefore, this pathway can be regarded as a nega-

REFERENCES

1. Arvanitis, D., and Davy, A. (2008) *Genes Dev.* **22,** 416–429
2. Pasquale, E. B. (2008) *Cell* **133,** 38–52
3. Nakamoto, M., Cheng, H. J., Friedman, G. C., McLaughlin, T., Hansen, M. J., Yoon, C. H., O'Leary, D. D., and Flanagan, J. G. (1996) *Cell* **86,** 755–766
4. Flanagan, J. G. (2006) *Curr. Opin. Neurobiol.* **16,** 59–66
5. Cheng, H. J., and Flanagan, J. G. (1994) *Cell* **79,** 157–168
6. Cheng, H., Govindan, J. A., and Greenstein, D. (2008) *Curr. Biol.* **18,** 705–714
7. Le Borgne, R. (2006) *Curr. Opin. Cell Biol.* **18,** 213–222
8. Gauthier, L. R., and Robbins, S. M. (2003) *Life Sci.* **74,** 207–216
9. Hancock, J. F. (2006) *Nat. Rev. Mol. Cell Biol.* **7,** 456–462
10. Mishra, S., and Joshi, P. G. (2007) *J. Neurochem.* **103,** Suppl. 1, 135–142
11. Davy, A., Gale, N. W., Murray, E. W., Klinghoffer, R. A., Soriano, P., Feuerstein, C., and Robbins, S. M. (1999) *Genes Dev.* **13,** 3125–3135
12. Lim, Y. S., McLaughlin, T., Sung, T. C., Santiago, A., Lee, K. F., and O'Leary, D. D. (2008) *Neuron* **59,** 746–758
13. Pereira, D. B., and Chao, M. V. (2007) *J. Neurosci.* **27,** 4859–4869
14. Ware, M. F., Tice, D. A., Parsons, S. J., and Lauffenburger, D. A. (1997)

J. Biol. Chem. **272,** 30185–30190

15. Mineo, C., Gill, G. N., and Anderson, R. G. (1999) *J. Biol. Chem.* **274,** 30636–30643

16. Kasai, A., Shima, T., and Okada, M. (2005) *Genes Cells* **10,** 1175–1187

17. Hoe, H. S., Minami, S. S., Makarova, A., Lee, J., Hyman, B. T., Matsuoka, Y., and Rebeck, G. W. (2008) *J. Biol. Chem.* **283,** 6288–6299

18. Gampel, A., Moss, L., Jones, M. C., Brunton, V., Norman, J. C., and Mellor, H. (2006) *Blood* **108,** 2624–2631

19. Hattori, M., Osterfield, M., and Flanagan, J. G. (2000) *Science* **289,** 1360–1365

20. Fusaki, N., Semba, K., Katagiri, T., Suzuki, G., Matsuda, S., and Yamamoto, T. (1994) *Int. Immunol.* **6,** 1245–1255

21. Takeuchi, M., Kuramochi, S., Fusaki, N., Nada, S., Kawamura-Tsuzuku, J., Matsuda, S., Semba, K., Toyoshima, K., Okada, M., and Yamamoto, T. (1993) *J. Biol. Chem.* **268,** 27413–27419

22. Kiyokawa, E., Baba, T., Otsuka, N., Makino, A., Ohno, S., and Kobayashi, T. (2005) *J. Biol. Chem.* **280,** 24072–24084

23. Flanagan, J. G., Cheng, H. J., Feldheim, D. A., Hattori, M., Lu, Q., and Vanderhaeghen, P. (2000) *Methods Enzymol.* **327,** 19–35

24. Morimura, T., Hattori, M., Ogawa, M., and Mikoshiba, K. (2005) *J. Biol. Chem.* **280,** 16901–16908

25. Bligh, E. G., and Dyer, W. J. (1959) *Can. J. Biochem. Physiol.* **37,** 911–917

26. Dittmer, J. C., and Lester, R. L. (1964) *J. Lipid Res.* **15,** 126–127

27. Ishitsuka, R., Yamaji-Hasegawa, A., Makino, A., Hirabayashi, Y., and Kobayashi, T. (2004) *Biophys. J.* **86,** 296–307

28. Wang, E., Norred, W. P., Bacon, C. W., Riley, R. T., and Merrill, A. H., Jr. (1991) *J. Biol. Chem.* **266,** 14486–14490

29. Chatterjee, S., Smith, E. R., Hanada, K., Stevens, V. L., and Mayor, S. (2001) *EMBO J.* **20,** 1583–1592

30. Rijnboutt, S., Jansen, G., Posthuma, G., Hynes, J. B., Schornagel, J. H., and Strous, G. J. (1996) *J. Cell Biol.* **132,** 35–47

31. Fivaz, M., Vilbois, F., Thurnheer, S., Pasquali, C., Abrami, L., Bickel, P. E., Parton, R. G., and van der Goot, F. G. (2002) *EMBO J.* **21,** 3989–4000

32. Sabharanjak, S., Sharma, P., Parton, R. G., and Mayor, S. (2002) *Dev. Cell* **2,** 411–423

33. Helms, J. B., and Zurzolo, C. (2004) *Traffic* **5,** 247–254

34. Mayor, S., and Riezman, H. (2004) *Nat. Rev. Mol. Cell Biol.* **5,** 110–120

35. Galvan, C., Camoletto, P. G., Cristofani, F., Van Veldhoven, P. P., and Ledesma, M. D. (2008) *Mol. Biol. Cell* **19,** 509–522

36. Ishitsuka, R., Sato, S. B., and Kobayashi, T. (2005) *J. Biochem.* **137,** 249–254

37. Marchesini, N., and Hannun, Y. A. (2004) *Biochem. Cell Biol.* **82,** 27–44

38. Tafesse, F. G., Ternes, P., and Holthuis, J. C. (2006) *J. Biol. Chem.* **281,** 29421–29425

39. Clarke, C. J., Snook, C. F., Tani, M., Matmati, N., Marchesini, N., and Hannun, Y. A. (2006) *Biochemistry* **45,** 11247–11256

40. Huitema, K., van den Dikkenberg, J., Brouwers, J. F., and Holthuis, J. C. (2004) *EMBO J.* **23,** 33–44

41. Tafesse, F. G., Huitema, K., Hermansson, M., van der Poel, S., van den Dikkenberg, J., Uphoff, A., Somerharju, P., and Holthuis, J. C. (2007) *J. Biol. Chem.* **282,** 17537–17547

42. Chudakova, D. A., Zeidan, Y. H., Wheeler, B. W., Yu, J., Novgorodov, S. A., Kindy, M. S., Hannun, Y. A., and Gudz, T. I. (2008) *J. Biol. Chem.* **283,** 28806–28816

43. Arnaud, L., Ballif, B. A., Forster, E., and Cooper, J. A. (2003) *Curr. Biol.* **13,** 9–17

44. Bock, H. H., and Herz, J. (2003) *Curr. Biol.* **13,** 18–26

45. Grimm, M. O., Grimm, H. S., Patzold, A. J., Zinser, E. G., Halonen, R., Duering, M., Tschape, J. A., De Strooper, B., Muller, U., Shen, J., and Hartmann, T. (2005) *Nat. Cell Biol.* **7,** 1118–1123

46. Goldshmit, Y., McLenachan, S., and Turnley, A. (2006) *Brain Res. Rev.* **52,** 327–345